



저작자표시-비영리-변경금지 2.0 대한민국

이용자는 아래의 조건을 따르는 경우에 한하여 자유롭게

- 이 저작물을 복제, 배포, 전송, 전시, 공연 및 방송할 수 있습니다.

다음과 같은 조건을 따라야 합니다:



저작자표시. 귀하는 원저작자를 표시하여야 합니다.



비영리. 귀하는 이 저작물을 영리 목적으로 이용할 수 없습니다.



변경금지. 귀하는 이 저작물을 개작, 변형 또는 가공할 수 없습니다.

- 귀하는, 이 저작물의 재이용이나 배포의 경우, 이 저작물에 적용된 이용허락조건을 명확하게 나타내어야 합니다.
- 저작권자로부터 별도의 허가를 받으면 이러한 조건들은 적용되지 않습니다.

저작권법에 따른 이용자의 권리는 위의 내용에 의하여 영향을 받지 않습니다.

이것은 [이용허락규약\(Legal Code\)](#)을 이해하기 쉽게 요약한 것입니다.

[Disclaimer](#)

Thesis for the Degree of Master of Science

Synthesis and Structures of Copper(II)
Complexes with Tetraaza Macrocycles



by

Taeyeong Kim

Department of Chemistry

The Graduate School

Pukyong National University

August 25, 2017

Synthesis and Structures of Copper(II)
Complexes with Tetraaza Macrocycles

(테트라아자 거대고리 구리(II)
착물의 합성 및 구조)



Advisor: Prof. Ju Chang Kim

by
Taeyeong Kim

A thesis submitted in partial fulfillment of the requirements
for the degree of

Master of Science

in Department of Chemistry, The Graduate School,
Pukyong National University

August 2017

**Synthesis and Structures of Copper(II) Complexes with
Tetraaza Macrocycles**

A thesis
by
Taeyeong Kim

Approved by:

(Chairman) Sang Yong Pyun

(Member) Yong-Cheol Kang

(Member) Ju Chang Kim

August 25, 2017

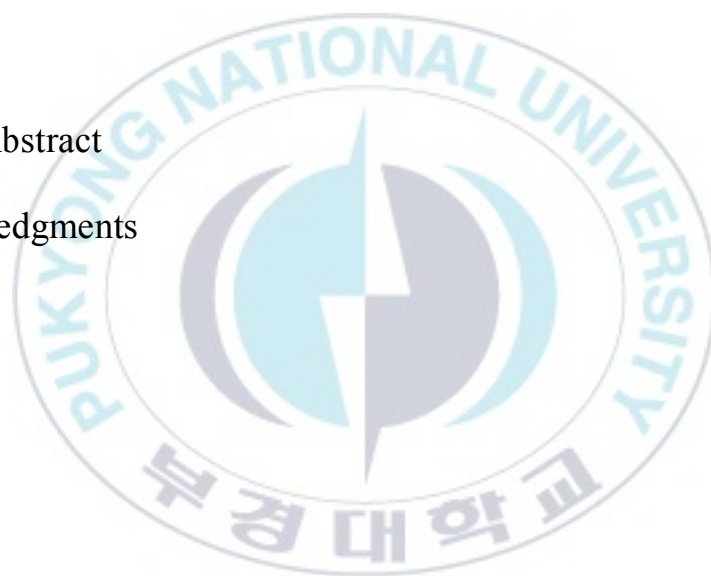
Table of Contents

List of Tables	iii
List of Figures	iv
Abstract	vii
General Introduction	1
References	3
CHAPTER I. Macrocyclic Copper(II) Complex with 1,2,4,5-Benzenetetracarboxylate Ligand	
Abstract	4
Introduction	5
Experimental	6
Result and Discussion	10
References	22

CHAPTER II. Supramolecules Self-Assembled by Copper(II)

Macrocycles with Muconic acid

Abstract	24
Introduction	25
Experimental	26
Result and Discussion	30
References	43
Korean Abstract	44
Acknowledgments	45



List of Tables

Table 1.1	Crystal data and structure refinement parameters of [Cu(L1)(H ₂ O) ₂][Cu ₂ (L1) ₂ (μ-btc ⁴⁻)]. 2ClO ₄ ·6H ₂ O·1.454CH ₃ CN (1)	9
Table 1.2	Selected bond distances (Å) and angles (°) for [Cu(L1)(H ₂ O) ₂][Cu ₂ (L1) ₂ (μ-btc ⁴⁻)]. 2ClO ₄ ·6H ₂ O·1.454CH ₃ CN (1)	15
Table 1.3	Hydrogen bonds for [Cu(L1)(H ₂ O) ₂][Cu ₂ (L1) ₂ (μ-btc ⁴⁻)]. 2ClO ₄ ·6H ₂ O·1.454CH ₃ CN (1) [Å and °]	16
Table 2.1	Crystal data and structure refinement parameters of [Cu(L1)(H ₂ O)]·(muco ²⁻)·(H ₂ O) ₄ (2) and [Cu(L2)(H ₂ O)]·(muco ²⁻)·(H ₂ O) ₇ (3)	29
Table 2.2	Selected bond distances (Å) and angles (°) for [Cu(L1)(H ₂ O)]·(muco ²⁻)·(H ₂ O) ₄ (2)	34
Table 2.3	Hydrogen bonds for [Cu(L1)(H ₂ O)]·(muco ²⁻)·(H ₂ O) ₄ (2) [Å and °]	35
Table 2.4	Selected bond distances (Å) and angles (°) for [Cu(L2)(H ₂ O)]·(muco ²⁻)·(H ₂ O) ₇ (3)	38
Table 2.5	Hydrogen bonds for [Cu(L2)(H ₂ O)]·(muco ²⁻)·(H ₂ O) ₇ (3) [Å and °]	39

List of Figures

- Figure 1.1 Molecular structure of $[\text{Cu}(\mathbf{L1})(\text{H}_2\text{O})_2][\text{Cu}_2(\mathbf{L1})_2(\mu\text{-btc}^{4-})] \cdot 2\text{ClO}_4 \cdot 6\text{H}_2\text{O} \cdot 1.454\text{CH}_3\text{CN}$ (**1**) with atom-labeling scheme. Hydrogen atoms other than those participating in hydrogen bonding, water molecules and acetonitrile molecules are omitted for clarity. 12
- Figure 1.2 Intermolecular interaction for $[\text{Cu}(\mathbf{L1})(\text{H}_2\text{O})_2][\text{Cu}_2(\mathbf{L1})_2(\mu\text{-btc}^{4-})] \cdot 2\text{ClO}_4 \cdot 6\text{H}_2\text{O} \cdot 1.454\text{CH}_3\text{CN}$ (**1**). Hydrogen atoms are omitted for clarity. 12
- Figure 1.3 Space-filling diagram (a) and extended molecular structure of $[\text{Cu}(\mathbf{L1})(\text{H}_2\text{O})_2][\text{Cu}_2(\mathbf{L1})_2(\mu\text{-btc}^{4-})] \cdot 2\text{ClO}_4 \cdot 6\text{H}_2\text{O} \cdot 1.454\text{CH}_3\text{CN}$ (**1**) (b) illustrating a 1D chain. Hydrogen atoms are omitted for clarity. 13
- Figure 1.4 Extended structure of (a) illustrating double strand by 1D chain. Packing diagram of $[\text{Cu}(\mathbf{L1})(\text{H}_2\text{O})_2][\text{Cu}_2(\mathbf{L1})_2(\mu\text{-btc}^{4-})] \cdot 2\text{ClO}_4 \cdot 6\text{H}_2\text{O} \cdot 1.454\text{CH}_3\text{CN}$ (**1**) (b). 14
- Figure 1.5 Infrared spectrum of $[\text{Cu}(\mathbf{L1})(\text{H}_2\text{O})_2][\text{Cu}_2(\mathbf{L1})_2(\mu\text{-btc}^{4-})] \cdot 2\text{ClO}_4 \cdot 6\text{H}_2\text{O} \cdot 1.454\text{CH}_3\text{CN}$ (**1**) [Nujol mull]. 18
- Figure 1.6 Electronic spectrum for $[\text{Cu}(\mathbf{L1})(\text{H}_2\text{O})_2][\text{Cu}_2(\mathbf{L1})_2(\mu\text{-btc}^{4-})] \cdot 2\text{ClO}_4 \cdot 6\text{H}_2\text{O} \cdot 1.454\text{CH}_3\text{CN}$ (**1**) in DMF. 19

Figure 1.7	Thermogravimetric analysis of [Cu(L1)(H ₂ O) ₂][Cu ₂ (L1) ₂ (μ-btc ⁴⁺)]· 2ClO ₄ ·6H ₂ O·1.454CH ₃ CN (1).	20
Figure 2.1	Molecular structure of [Cu(L1)(H ₂ O)]·(muco ²⁻)·(H ₂ O) ₄ (2) with atom-labeling scheme. Hydrogen atoms other than those participating in hydrogen bonding are omitted for clarity.	32
Figure 2.2	Space-filling diagram of [Cu(L1)(H ₂ O)]·(muco ²⁻)·(H ₂ O) ₄ (2).	32
Figure 2.3	2D supramolecular sheet of [Cu(L1)(H ₂ O)]·(muco ²⁻)·(H ₂ O) ₄ (2) with atom-labeling scheme. Hydrogen atoms other than those participating in hydrogen bonding are omitted for clarity.	33
Figure 2.4	2D supramolecular layer of [Cu(L1)(H ₂ O)]·(muco ²⁻)·(H ₂ O) ₄ (2) with atom-labeling scheme. Hydrogen atoms other than those participating in hydrogen bonding are omitted for clarity.	33
Figure 2.5	Molecular structure of [Cu(L2)(H ₂ O)]·(muco ²⁻)·(H ₂ O) ₇ (3) with atom-labeling scheme. Hydrogen atoms other than those participating in hydrogen bonding are omitted for clarity.	36
Figure 2.6	Space-filling diagram of [Cu(L2)(H ₂ O)]·(muco ²⁻)·(H ₂ O) ₇ (3).	36

- Figure 2.7 2D supramolecular sheet of $[\text{Cu}(\mathbf{L2})(\text{H}_2\text{O})] \cdot (\text{muco}^{2-}) \cdot (\text{H}_2\text{O})_7$ (**3**) with atom-labeling scheme. Hydrogen atoms other than those participating in hydrogen bonding are omitted for clarity. 37
- Figure 2.8 2D supramolecular layer of $[\text{Cu}(\mathbf{L2})(\text{H}_2\text{O})] \cdot (\text{muco}^{2-}) \cdot (\text{H}_2\text{O})_7$ (**3**) with atom-labeling scheme. Hydrogen atoms other than those participating in hydrogen bonding are omitted for clarity. 37
- Figure 2.9 Infrared spectra of (a) $[\text{Cu}(\mathbf{L1})(\text{H}_2\text{O})] \cdot (\text{muco}^{2-}) \cdot (\text{H}_2\text{O})_4$ (**2**), and (b) $[\text{Cu}(\mathbf{L2})(\text{H}_2\text{O})] \cdot (\text{muco}^{2-}) \cdot (\text{H}_2\text{O})_7$ (**3**) [Nujol mull]. 41
- Figure 2.10 Electronic spectra for (a) $[\text{Cu}(\mathbf{L1})(\text{H}_2\text{O})] \cdot (\text{muco}^{2-}) \cdot (\text{H}_2\text{O})_4$ (**2**), and (b) $[\text{Cu}(\mathbf{L2})(\text{H}_2\text{O})] \cdot (\text{muco}^{2-}) \cdot (\text{H}_2\text{O})_7$ (**3**) in DMF. 42

Syntheses and Structures of Copper(II) Complexes with Tetraaza Macrocycles

Taeyeong Kim

*Department of science, Graduate School,
Pukyong National University*

Abstract

Three new copper(II) complexes with the composition $[\text{Cu}(\mathbf{L1})(\text{H}_2\text{O})_2][\text{Cu}_2(\mathbf{L1})_2(\mu\text{-btc}^{4-})] \cdot 2\text{ClO}_4 \cdot 6\text{H}_2\text{O} \cdot 1.454\text{CH}_3\text{CN}$ (1), $[\text{Cu}(\mathbf{L1})(\text{H}_2\text{O})] \cdot (\text{muco}^{2-}) \cdot (\text{H}_2\text{O})_4$ (2), $[\text{Cu}(\mathbf{L2})(\text{H}_2\text{O})] \cdot (\text{muco}^{2-}) \cdot (\text{H}_2\text{O})_7$ (3) (\mathbf{L} = 3,14-dimethyl-2,6,13,17-tetraazatricyclo[14.4.0^{1.18}.0^{7.12}]docosane, H_4btc = 1,2,4,5-benzenetetracarboxylic acid, H_2muco = *trans,trans*-muconic acid) have been synthesized and structurally characterized by a combination of analytical, spectroscopic and X-ray crystallography. In (1), two different copper(II) coordination geometries, a five-coordinate square pyramid as well as an axially elongated six – coordinate octahedron, and (2), (3) have a similar structures, but different arrangements, are observed. In all complexes various types of hydrogen bonding interactions play an important role in determining the shapes of structural geometries, respectively.

General Introduction

In recent years supramolecules have moved from narrow fields to the focus of common interest. Supramolecules based on intermolecular interactions, such as hydrogen bond, C-H \cdots π interactions, $\pi\cdots\pi$ interactions, etc., of transition metal ions and ligands and therefore are of interest due to their structural diversities and potential applications such as bioactivity, catalysis, medicine, molecular magnetism, gas storage or sensitization [1-7]. The application of supramolecular concepts such molecular recognition and self-assembly offers an approach to crystal engineering. Compared with free metal ions, metal complex of tetraazamacrocycle have filled equatorial sites and empty axial sites for incoming ligands. Consequently, the bridging ligands which interacted with tetraazamacrocycles complex can easily be anticipated and controlled by the generation of metallosupramolecules. With all these advantages, metal complex of tetraazamacrocycle has relatively been unexplored as building blocks for assembly of metallosupramolecules.

The bridging ligand plays the important roles that an effects on the structures of the supramolecules. Multidentate polycarboxylates are well-known versatile ligands which can bridge metal ions, leading to the formation of polynuclear system. Further, the remaining carboxylic acid groups that are not coordinated to metal ions are able to act as hydrogen bond donors and/or acceptors for the extension of molecular units. Especially, tetraazamacrocyclic complexes with multi-connecting ligands have been demonstrated to be good building blocks for the construction of multi-dimensional

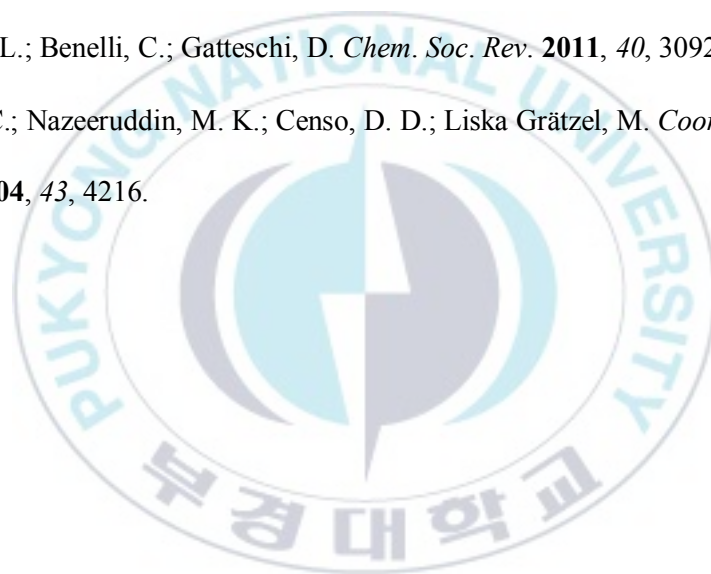
supramolecular networks.

On the basis of the foregoing, Multi-dimensional transition metal complexes with tetraazamacrocyclic ligands and polycarboxylate ligands have been constructed in this thesis. The syntheses and properties of three new macrocyclic copper(II) supramolecules have been described in this work.

This thesis is composed of two chapters. In the Chapter I, the syntheses and properties of one new macrocyclic copper(II) supramolecule with bridging btc^{4-} (H_4btc = 1,2,4,5-benzenetetracarboxylic acid) ligands is reported. In the Chapter II, syntheses and properties of two new macrocyclic copper(II) supramolecules containing muco^{2-} (H_2muco = *trans,trans*-muconic acid) are reported. The details of the structures for the new complexes were determined by analytical, spectroscopic, and X-ray diffraction methods.

References

- [1] Winter, A.; Schubert, U. S. *Chem.Soc. Rev.* **2016**, *45*, 5311.
- [2] Suh, M. P.; Cheon, Y. Y.; Lee, Y. Y. *Coord. Chem. Rev.* **2008**, *252*, 1007.
- [3] Janiak, C.; *Dalton Trans.* **2003**, 2781.
- [4] Eryazici, I.; Moorefield, C. N.; Newkome, G. R. *Chem. Rev.* **2008**, *108*, 1834.
- [5] Liu, H.-K.; Sadler, P. J. *Acc. Chem. Res.* **2011**, *44*, 349.
- [6] Sorace, L.; Benelli, C.; Gatteschi, D. *Chem. Soc. Rev.* **2011**, *40*, 3092.
- [7] Klein, C.; Nazeeruddin, M. K.; Censo, D. D.; Liska Grätzel, M. *Coord. Chem. Rev.* **2004**, *43*, 4216.



CHAPTER I

Macrocyclic Copper(II) Complex with 1,2,4,5-Benzenetetracarboxylate Ligation

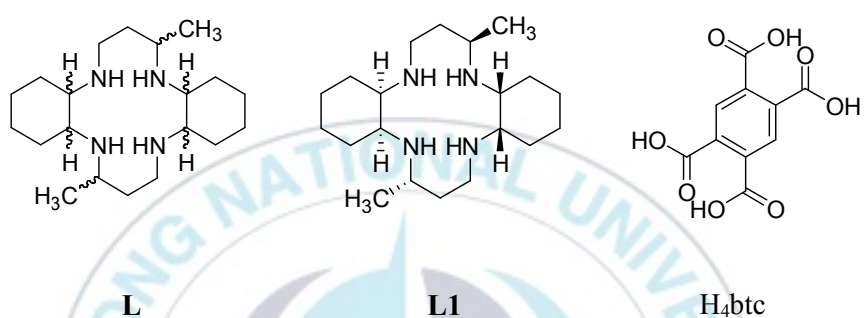
Abstract

The new Copper(II) complex, $[\text{Cu}(\mathbf{L1})(\text{H}_2\text{O})_2][\text{Cu}_2(\mathbf{L1})_2(\mu\text{-btc}^{4-})] \cdot 2\text{ClO}_4 \cdot 6\text{H}_2\text{O} \cdot 1.454\text{CH}_3\text{CN}$ (**1**) ($\mathbf{L} = 3,14\text{-dimethyl-}2,6,13,17\text{-tetraazatricyclo}[14.4.0^{1.18}.0^{7.12}]$ docosane, $\text{H}_4\text{btc} = 1,2,4,5\text{-benzenetetracarboxylic acid}$) was prepared by the reaction of $[\text{Cu}(\mathbf{L})](\text{ClO}_4)_2$ and btcH_4 in $\text{DMF}/\text{H}_2\text{O}/\text{CH}_3\text{CN}/\text{NEt}_3$. The complex **1** was characterized by a combination of analytical, spectroscopic techniques. In addition, molecular structure was determined by single crystal X-ray diffraction methods. In **1**, two different copper(II) coordination geometries, a five-coordinate square pyramid as well as an axially elongated six-coordinate octahedron, are observed. The btc^{4-} ligand bridges two copper(II) macrocycles to form a dimer where all the hydrogen atoms of H_4btc were deprotonated, forming a complex dianion. Additional copper(II) macrocycle involves in **1** in which two aqua ligands interact with central metal ion weakly, resulting in the formation of complex dication. Thus, the whole complex **1** is charge balanced.

Introduction

Self-assembled metal complexes with characteristic network topologies have been of enormous interest due to their potential properties in supramolecular chemistry. Especially, the transition metal complexes with polycarboxylate ligand have attracted great attention due to their interesting structures and potential applications [1-3]. Recently, macrocyclic complexes and aromatic polycarboxylate ligands with two or more metal binding sites have been found to be good building blocks for the construction of multi-dimensional supramolecular networks [2,4-10]. Among the aromatic polycarboxylate ligands, H_4btc is suitable of interest for the study of complexes with various coordination and multi-dimension complexes with metal because H_4btc has following interesting features [9,11,12]. H_4btc contains four carboxyl groups which can be partially or fully deprotonated, inducing interesting structures with multi-dimensions and it can act only as hydrogen bond donors but also as hydrogen bond acceptors through inter and/or intra molecular fashion, depending on the degree of deprotonated carboxyl groups. Thus, the H_4btc may be a good choice for the preparation of structurally interesting supramolecule. There have been several reports that the diverse shapes H_4btc , H_3btc^- , H_2btc^{2-} in which the shapes vary with the types of hydrogen bond and the degree of deprotonation. [13-16]. However, the examples of macrocyclic transition metal complexes formed with the completely deprotonated btc^{4-} ligands are rarely observed. Here, the novel 1D copper(II) is synthesized and described by the reaction between the copper(II) macrocyclic

complex $[\text{Cu}(\text{L1})](\text{ClO}_4)_2$ and the H_4btc . In complex **1**, various types of hydrogen bonding interactions play an important role to determine the copper(II) coordination geometries as well as the shape of the btc^{4-} anions. The details of the synthesis, structures, and properties of **1** is discussed in this report.



Experimental

Material and methods

All chemicals utilized in this investigation were obtained from commercial sources and were used without further purification. Distilled water used for all procedures. Infrared spectrum of solid sample was recorded on JASCO FT-IR-4000 spectrophotometer between 4000 and 400 cm^{-1} as Nujol mulls on KBr discs. Thermogravimetric analysis was performed on a Perkin-Elmer Model TGA-7 under an air sweep from 50 to 850 $^{\circ}\text{C}$ at a heating rate of 10 $^{\circ}\text{C}/\text{min}$. Electronic spectrum

using sample diluted with DMF was recorded with a Shimadzu UV-2600 recording spectrophotometer. Elemental analyses were performed on VarioMICRO. The precursor complex [Cu(L1)](ClO₄)₂ was synthesized by previously reported methods [17].

Synthesis of 1

To a mixture of DMF and acetonitrile (1:1 v/v) solution (30mL) of [Cu(L1)](ClO₄)₂ (240 mg, 0.4 mmol) was added an aqueous solution of 1,2,4,5-benzentetracarboxylic acid (102 mg, 0.4 mmol) and 1mL of triethylamine in an open beaker at ambient condition. Purple crystals of **1** were obtained in a week. Suitable crystals of **1** for X-ray diffraction studies and subsequent spectroscopic measurements were manually collected under the microscope. Anal. Calc. for C_{72.91}H_{142.36}Cl₂Cu₃N_{13.45}O₂₄ (**1**): C, 47.25 %; H, 7.69 %; N, 10.17 %. Found: C, 46.87 %; H, 5.35 %; N, 9.67 %.

X-ray crystallography

A summary of selected crystallographic data for **1** is given in Table 1.1 X-ray data were collected on a Nonius Kappa CCD diffractometer, using graphite monochromated Mo K α radiation ($\lambda=0.71073$ Å). A combination of $1^\circ\Phi$ and Ω (with κ offsets) scans were used to collect sufficient data. The data frames were integrated and scaled using the DENZO-SMN package. The structure was solved and refined

using the SHELXTL-2014/7 package. Refinement was by full-matrix least squares on F^2 , using all data (negative intensities included). Hydrogen atoms were included in calculated position. There are two different types of discrete centrosymmetric copper(II) macrocycles, five waters and one acetonitrile in the formula unit. Only the two unique water molecules are shown in Figure 1.1. The dication is linked to the dianion by hydrogen bond through acetonitrile and water molecules.



Table 1.1. Crystal data and structure refinement parameters of
 $[\text{Cu}(\mathbf{L1})(\text{H}_2\text{O})_2][\text{Cu}_2(\mathbf{L1})_2(\mu\text{-btc}^4)] \cdot 2\text{ClO}_4 \cdot 6\text{H}_2\text{O} \cdot 1.454\text{CH}_3\text{CN}$ (**1**)

	1
Empirical formula	$\text{C}_{72.91} \text{H}_{142.36} \text{Cl}_2 \text{Cu}_3 \text{N}_{13.45} \text{O}_{24}$
Formula weight	1853.09
Temperature (K)	150(2)
Wavelength (Å)	0.71073
Crystal system	Triclinic
Space group	P-1
a (Å)	9.3618(8)
b (Å)	13.8049(11)
c (Å)	17.9693(15)
α (°)	68.000(2)
β (°)	78.583(2)
γ (°)	86.534(2)
Volume (Å ³)	2110.4(3)
Z	1
$D_{\text{calc.}}$ (Mg/m ³)	1.458
Absorption coefficient (mm ⁻¹)	0.894
Crystal size (mm ³)	987
θ range for data collection	1.245 to 27.630°
Index ranges	-12 ≤ h ≤ 12 -17 ≤ k ≤ 17 -23 ≤ l ≤ 23
Reflections collected	52648
Independent reflections	9762 [R(int) = 0.0336]
Completeness to θ	100.0 % ($\theta = 25.242^\circ$)
Absorption correction	Semi-empirical from equivalents
Max. and min. transmission	0.7456 and 0.6751
Data / restraints / parameter	9762 / 0 / 553
Goodness-of-fit on F^2	1.049
Final R indices [$I > 2\sigma(I)$]	R1 = 0.0355 wR2 = 0.0846
R indices (all data)	R1 = 0.476 wR2 = 0.0933
Largest diff. peak and hole	0.726 and -0.724 e. Å ⁻³

Results and Discussion

Description of structure of 1

The purple complex **1** was obtained by reacting $[\text{Cu}(\mathbf{L1})(\text{ClO}_4)_2]$ with H_4btc in DMF/ $\text{CH}_3\text{CN}/\text{H}_2\text{O}$, followed by slow evaporation at ambient temperature of the resulting solution. The complex **1** was fairly stable in air and almost insoluble in DMF, CH_3CN or H_2O . Figure 1.1 shows the molecular structure of **1**. The structure of **1** is made up of a macrocyclic diaqua copper(II) complex dication $[\text{Cu}(\mathbf{L})(\text{H}_2\text{O})_2]$ and macrocyclic dimeric copper(II) complex dianion $[\text{Cu}_2(\mathbf{L})_2(\mu\text{-btc}^{4-})]$. Two aqua ligands sit on the copper(II) ion axially in the complex, where the hydrogen bonds play role in supporting the coordination of water molecules to the copper(II) ion (Table 1.3). As usual, the macrocyclic ligand skeleton of **L** takes the most stable “*trans III* (R,R,S,S)” conformation. The Cu-N distances were 2.0613(17), 2.2013(16), 2.0479(17), 2.0105(16) Å and Cu-O distances was 2.3742(14) Å in the macrocyclic dimeric copper(II) complex dianion. These values fall within the range of comparable reports for such a geometry [19].

In the dianion, the btc^{4-} ligand bridged two copper(II) macrocycles to form a dimer, resulting in the structure of a five-coordinate square pyramid. In dication, an inversion center exists on the central copper(II) ion which is coordinated by the macrocyclic ligand **L1** and two aqua axial ligands, resulting in the structure of an

axially elongated octahedron. Although the free acid H_4btc is introduced during the synthesis of **1**, all of the carboxylic acids are deprotonated and the resulting btc^{4-} is bridged in the two copper macrocycles and resulting formed dimeic copper(II) complex dianion. Carboxylates in btc^{4-} is observed the hydrogen bonds between the pre-organized N-H groups of the macrocycles **L1** which are believed to be important for the design and development of copper(II) complexes having a strong Cu-O bond. Furthermore, btc^{4-} makes a hydrogen bond with the water molecules of the macrocyclic copper(II) dications to form a 1D supramolecular chain (Figure 1.3). The Cu-N distances of 2.0261(16), 2.0372(17) Å and Cu-O interatomic distance of 2.713 Å in the macrocyclic copper(II) dication are similar to those of octahedral macrocyclic copper(II) complexes [13-15]. Several interacted effects are existed to work for this long Cu-O interatomic distance. The Jahn-Teller effect is observed in this system, which indicates that the structure of copper(II) complex is distorted owing to the octahedral d^9 configuration. As well the intermolecular hydrogen bond between O(1W)-H(1WA)...O(4) and O(1W)-H(1WB)...O(2W) as found in **1** results in the weak Cu-O interaction.

The macrocyclic copper(II) dications are interacted to the macrocyclic copper(II) dianions by hydrogen bonds through water molecules and acetonitrile molecules. Finally, they are charge balanced.

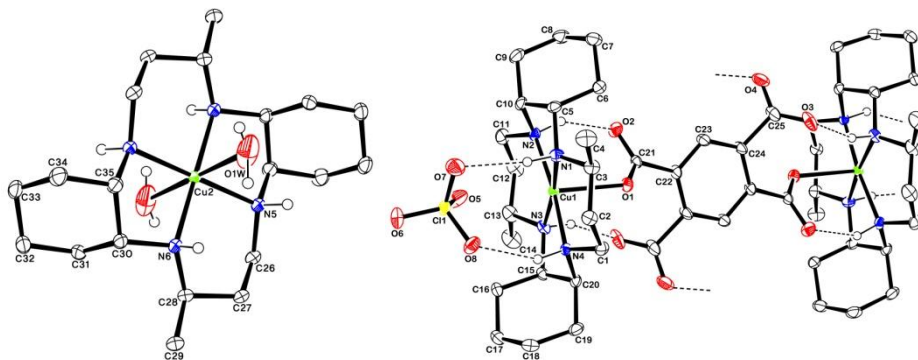


Figure 1.1. Molecular structure of

$[\text{Cu}(\mathbf{L1})(\text{H}_2\text{O})_2][\text{Cu}_2(\mathbf{L1})_2(\mu\text{-btc}^4)] \cdot 2\text{ClO}_4 \cdot 6\text{H}_2\text{O} \cdot 1.454\text{CH}_3\text{CN}$ (**1**) with atom-labeling scheme. Hydrogen atoms other than those participating in hydrogen bonding, water molecules and acetonitrile molecules are omitted for clarity.

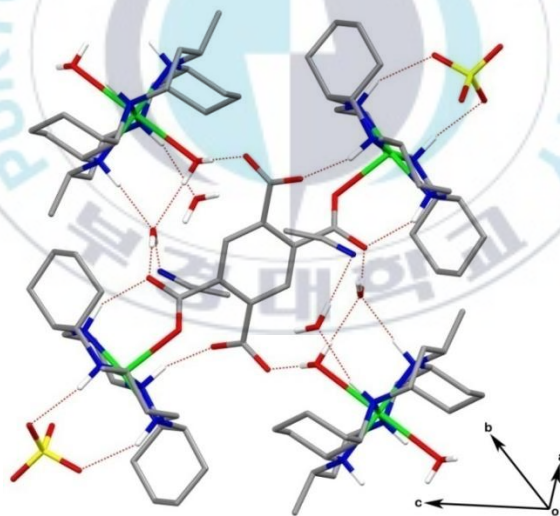


Figure 1.2. Intermolecular interaction for

$[\text{Cu}(\mathbf{L1})(\text{H}_2\text{O})_2][\text{Cu}_2(\mathbf{L1})_2(\mu\text{-btc}^4)] \cdot 2\text{ClO}_4 \cdot 6\text{H}_2\text{O} \cdot 1.454\text{CH}_3\text{CN}$ (**1**). Hydrogen atoms are omitted for clarity.

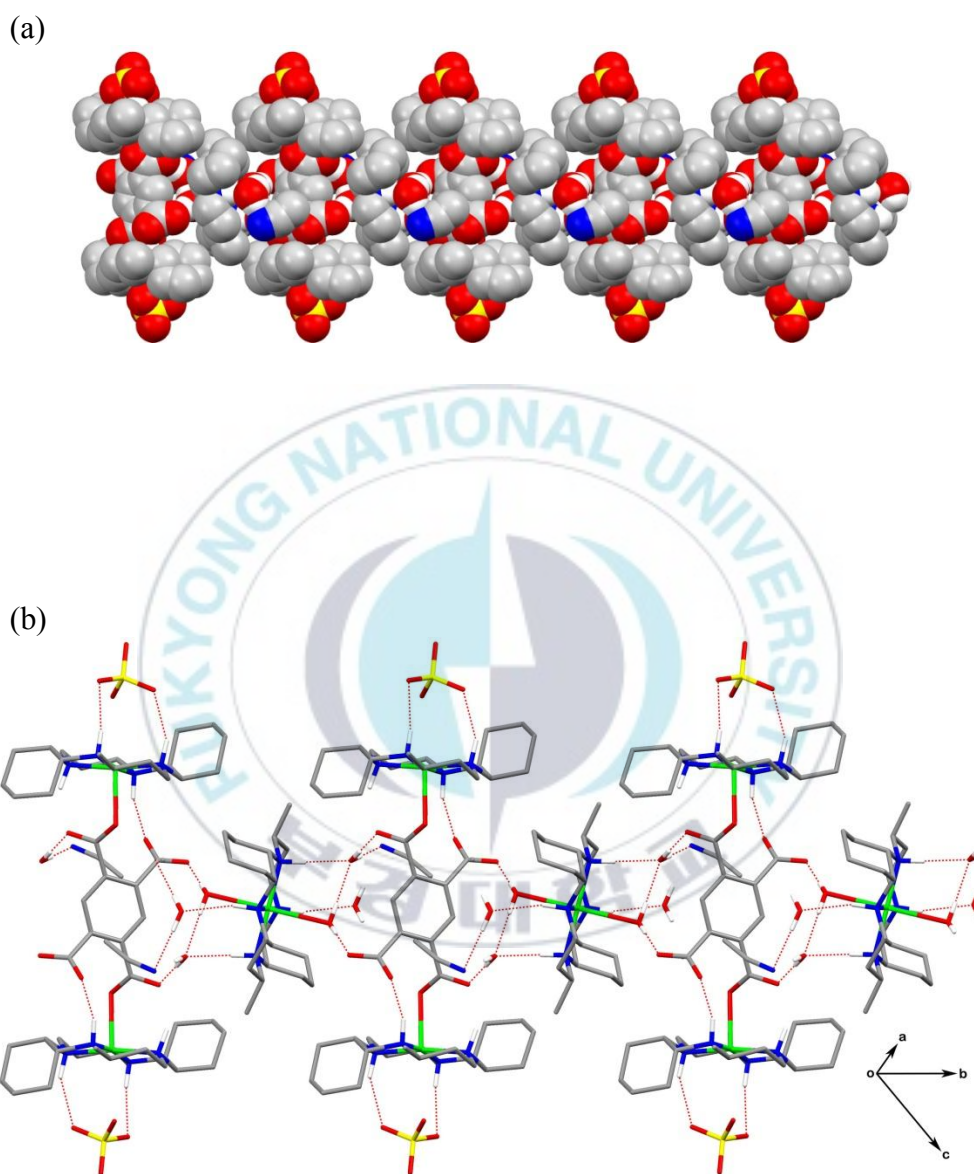


Figure 1.3. Space-filling diagram (a) and extended molecular structure of $[\text{Cu}(\mathbf{L1})(\text{H}_2\text{O})_2][\text{Cu}_2(\mathbf{L1})_2(\mu\text{-btc}^4)] \cdot 2\text{ClO}_4 \cdot 6\text{H}_2\text{O} \cdot 1.454\text{CH}_3\text{CN}$ (**1**) (b) illustrating a 1D chain. Hydrogen atoms are omitted for clarity.

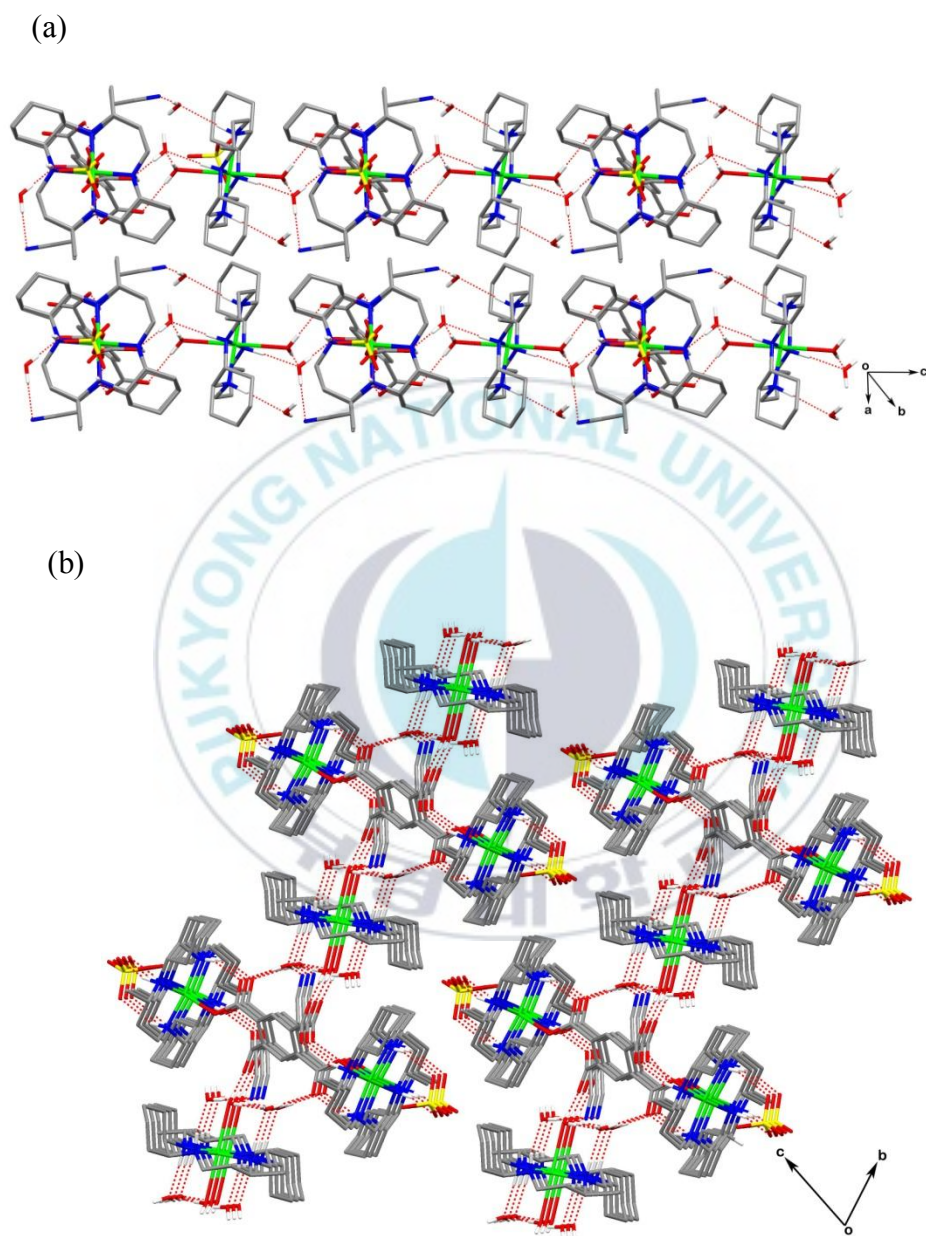


Figure 1.4. Extended structure of (a) illustrating double strand by 1D chain. Packing diagram of $[\text{Cu}(\mathbf{L1})(\text{H}_2\text{O})_2][\text{Cu}_2(\mathbf{L1})_2(\mu\text{-btc}^4)] \cdot 2\text{ClO}_4 \cdot 6\text{H}_2\text{O} \cdot 1.454\text{CH}_3\text{CN}$ (**1**) (b).

Table 1.2. Selected bond distances (Å) and angles (°) for
 $[\text{Cu}(\mathbf{L1})(\text{H}_2\text{O})_2][\text{Cu}_2(\mathbf{L1})_2(\mu\text{-btc}^4)] \cdot 2\text{ClO}_4 \cdot 6\text{H}_2\text{O} \cdot 1.454\text{CH}_3\text{CN}$ (**1**)

Cu(1)-N(4)	2.0105(16)	Cu(1)-N(2)	2.0213(16)
Cu(1)-N(3)	2.0479(17)	Cu(1)-N(1)	2.0613(17)
Cu(1)-O(1)	2.3742(14)	O(1)-C(21)	1.255(2)
O(2)-C(21)	1.262(3)	C(25)-O(4)	1.247(6)
C(25)-O(3)	1.260(6)	C(25)-C(24)	1.530(4)
C(21)-C(22)	1.513(3)	Cu(2)-N(5)	2.0261(16)
Cu(2)-N(6)	2.0372(17)		
N(4)-Cu(1)-N(3)	85.15(7)	N(2)-Cu(1)-N(3)	96.59(7)
N(4)-Cu(1)-N(1)	93.06(6)	N(2)-Cu(1)-N(1)	84.26(7)
N(4)-Cu(1)-O(1)	92.11(6)	N(2)-Cu(1)-O(1)	95.39(6)
N(3)-Cu(1)-O(1)	87.25(6)	N(1)-Cu(1)-O(1)	100.03(6)
N(5)-Cu(2)-N(6)	94.63(7)	N(5)#2-Cu(2)-N(6)	85.37(7)

Symmetry transformations used to generate equivalent atoms:

#1 $-x+1, -y+1, -z$ #2 $-x+1, -y+2, -z$

Table 1.3. Hydrogen bonds for[Cu(L1)(H₂O)₂][Cu₂(L1)₂(μ-btc⁴⁻)]·2ClO₄·6H₂O·1.454CH₃CN (**1**) [Å and °]

D-H...A	d(D-H)	d(H...A)	d(D...A)	<(DHA)
N(1)-H(1N)...Cl(1)	1.00	2.80	3.6652(19)	144.8
N(1)-H(1N)...O(7)	1.00	2.15	3.129(3)	164.6
N(2)-H(2N)...O(2)	1.00	1.94	2.848(2)	148.9
N(3)-H(3N)...O(3)#1	1.00	1.95	2.909(3)	159.5
N(3)-H(3N)...O(3A)#1	1.00	2.16	3.065(10)	150.1
N(4)-H(4N)...O(8)	1.00	2.23	3.147(2)	151.8
N(5)-H(5N)...O(3W)#1	1.00	2.23	3.205(3)	165.2
N(6)-H(6N)...O(2W)	1.00	1.95	2.953(3)	176.2
O(1W)-H(1WA)...O(4)	0.84	2.07	2.908(6)	179.2
O(1W)-H(1WA)...O(4A)	0.84	1.50	2.301(7)	159.6
O(1W)-H(1WB)...O(2W)	0.84	1.93	2.773(3)	178.5
O(2W)-H(2WB)...O(2)	0.84	1.83	2.670(2)	179.6
O(2W)-H(2WA)...N(1S)	0.84	1.94	2.780(9)	178.2
O(3W)-H(3WA)...O(4W)	0.84	2.02	2.778(5)	149.2
O(3W)-H(3WA)...O(5W)	0.84	2.18	3.018(5)	179.7
O(3W)-H(3WB)...N(1S)#1	0.84	1.92	2.758(7)	178.5

Symmetry transformations used to generate equivalent atoms:

#1 -x+1,-y+1,-z #2 -x+1,-y+2,-z

Spectroscopic properties and thermal analysis for 1

The solid state infrared spectrum of Figure 1.5 clearly shows the existence of the macrocyclic ligand, btcH₄ ligand, water molecules and perchlorate ions. The spectrum shows the stretching frequencies of the three different carboxyl groups at 1651, 1619 and 1561 cm⁻¹ for the $\nu_{as}(\text{COO})$ and 1411, 1320, 1239 cm⁻¹ for the $\nu_s(\text{COO})$. For the carboxylate groups, the separation between $\nu_{as}(\text{COO})$ and $\nu_s(\text{COO})$ of 150 cm⁻¹ is considerably less than the value of 200 cm⁻¹ for free carboxylate, indicative of a bidentate bridging carboxylate groups coordinated to the central copper ion [17]. Two weak bands at 3245 and 3156 cm⁻¹ can be assigned to the $\nu(\text{NH})$ of the macrocycle and the broad band at 3460 cm⁻¹ is designed $\nu(\text{OH})$ of the lattice water molecules. The presence of perchlorate ions for **1** was suggested by the very strong band at 1076 cm⁻¹ for the $\nu_{as}(\text{ClO})$ and 625 cm⁻¹ for the $\delta(\text{O-Cl-O})$. The solid state electronic spectrum of figure 1.6 is composed of two bands at 269 and 555 nm. The broad lower energy bands in the visible region are d-d transition, are attributed to a composite of the three possible transition for d_{xy} , d_{yz} , d_{zx} to $d_{x^2-y^2}$. The strong higher energy bands are assigned to ligand-metal charge transfer transitions related axial oxygen or macrocycle nitrogen donors. TGA curve for **1** shows a first weight loss of 2.1% (calculated 2.1%) over 100 – 200 °C, corresponding to the loss of two lattice water molecules. Final residues (observed 13.68%, calculated 13.68%) were remained above 400 °C with 3CuO composition.

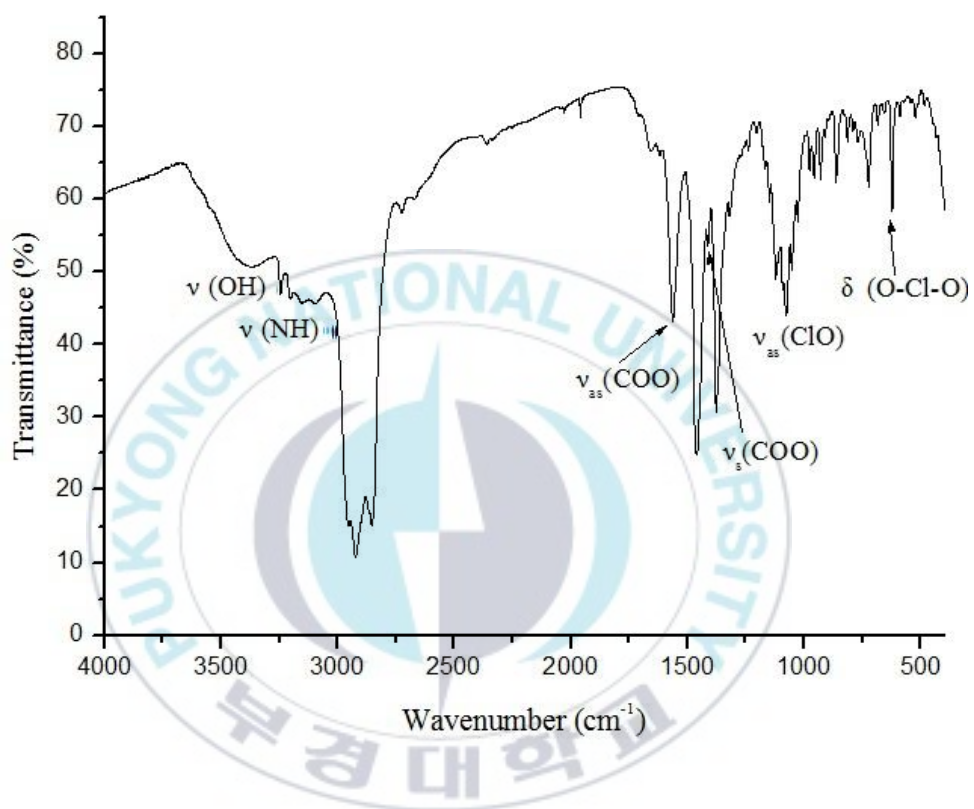


Figure 1.5. Infrared spectrum of $[\text{Cu}(\text{L1})(\text{H}_2\text{O})_2][\text{Cu}_2(\text{L1})_2(\mu\text{-btc}^4)] \cdot 2\text{ClO}_4 \cdot 6\text{H}_2\text{O} \cdot 1.454\text{CH}_3\text{CN}$ (1) [Nujol mull].

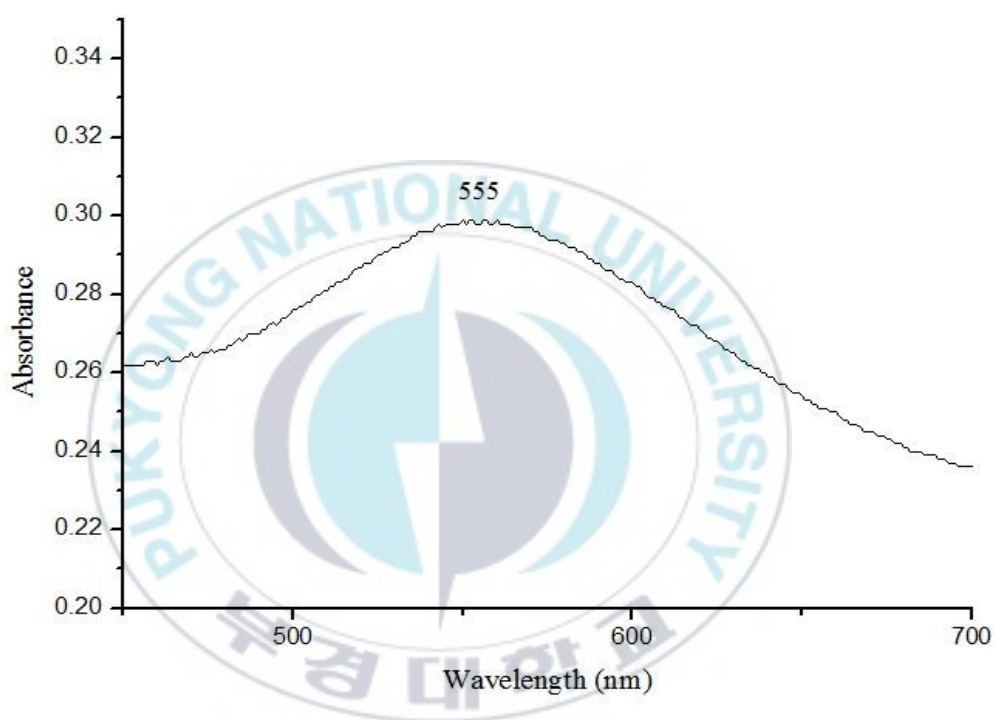


Figure 1.6. Electronic spectrum for

$[\text{Cu}(\mathbf{L1})(\text{H}_2\text{O})_2][\text{Cu}_2(\mathbf{L1})_2(\mu\text{-btc}^{4-})]\cdot 2\text{ClO}_4\cdot 6\text{H}_2\text{O}\cdot 1.454\text{CH}_3\text{CN}$ (**1**) in DMF.

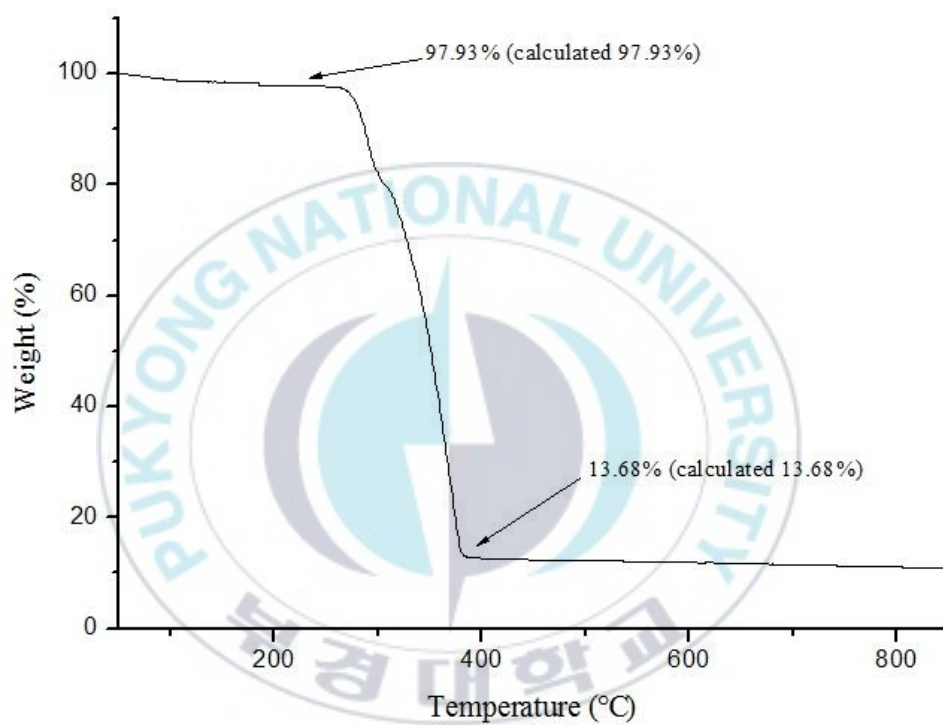


Figure 1.7. Thermogravimetric analysis of $[\text{Cu}(\mathbf{L1})(\text{H}_2\text{O})_2][\text{Cu}_2(\mathbf{L1})_2(\mu\text{-btc}^+)] \cdot 2\text{ClO}_4 \cdot 6\text{H}_2\text{O} \cdot 1.454\text{CH}_3\text{CN}$ (**1**).

In conclusion, the copper(II) complex $[\text{Cu}(\mathbf{L1})(\text{H}_2\text{O})_2][\text{Cu}_2(\mathbf{L1})_2(\mu\text{-btc}^{4-})] \cdot 2\text{ClO}_4 \cdot 6\text{H}_2\text{O} \cdot 1.454\text{CH}_3\text{CN}$ (**1**) has been prepared and structurally characterized. The complex **1** which contains the two different copper(II) coordination geometries, a five-coordinate square pyramid as well as an axially elongated six-coordinate octahedron, are observed. The btc^{4-} ligand bridges two copper(II) macrocycles to form a dimer where all the hydrogen atoms of btcH_4 were deprotonated, forming a complex dianion. Additional copper(II) macrocycle involves in (**1**) in which two aqua ligands interact with central metal ion weakly, resulting in the formation of complex dication. Lattice water and acetonitrile molecules are supported the retention of btc^{4-} by hydrogen bonding. The macrocyclic copper(II) dications and the macrocyclic copper(II) anions are linked through lattice water and acetonitrile molecules by hydrogen bonding to form a 1D supramolecular chain.

References

- [1] Eddaoudi, M.; Moler, D.B.; Li, H.; Chen, B.; Reineke, T.M.; O'Keeffe, M.; Yaghi, O.M. *Acc. Chem. Res.* **2001**, *34*, 319.
- [2] Choi, H. J.; Suh, M. P. *J. Am. Chem. Soc.* **1998**, *120*, 10622.
- [3] Choi, H.J.; Lee, T.S.; Suh, M.P. *Inorg. Chem.* **1999**, *38*, 6309.
- [4] Yaghi, O.M.; Li, H.; Davis, C.; Richardson, D.; Groy, T.L. *Acc. Chem. Res.* **1998**, *31*, 474.
- [5] Choi, K.-Y.; Chun, K.M.; Suh, I.-H. *Polyhedron* **2001**, *20*, 57.
- [6] Eddaoudi, M.; Kim, J.; O'Keeffe, M.; Yaghi, O.M. *J. Am. Chem. Soc.* **2002**, *124*, 376.
- [7] Rochon, F.D.; Massarweh, G. *Inorg. Chim.Acta* **2000**, *304*, 190.
- [8] Rochon, F.D.; Massarweh, G. *Inorg. Chim.Acta* **2001**, *314*, 163.
- [9] Shi, Q.; Cao, R.; Sun, D.-F.; Hong, M.-C.; Liang, Y.-C. *Polyhedron* **2001**, *20*, 3287.
- [10] Wu, L.P.; Munakata, M.; Kuroda-Sowa, T.; Maekawa, M.; Suenaga, Y. *Inorg. Chim.Acta* **1996**, *249*, 183.
- [11] Biradha, K.; Zaworotko, M.J. *Cryst. Eng.* **1998**, *1*, 67.
- [12] Moulton, B.; Zaworotko, M.J. *Chem. Rev.* **2001**, *101*, 1629.
- [13] Kim, J.C.; Lough, A.J.; Jo, H. *Inorg. Chem. Commun.* **2002**, *5*, 616.
- [14] Kim, J.C.; Jo, H.; Lough, A.J.; Cho, J.; Lee, U.; Pyun, S.Y. *Inorg. Chem. Commun.* **2003**, *6*, 474.

- [15] Kim, J.C.; Lough, A.J.; Kim, H. *Inorg. Chem. Commun.* **2002**, *5*, 771.
- [16] Cho, J.; Lough, A.J.; Kim, J.C. *Inorg. Chim. Acta* **2003**, *342*, 305.
- [17] Kang, S.-G.; Kweon, J.K.; Jung, S.-K. *Bull. Korean Chem. Soc.* **1991**, *12*, 483.
- [18] Li, M.-X.; Xie, G.-Y.; Jin, S.-L.; Gu, Y.-D.; Chen, M.-Q.; Liu, J.; Xu, Z.; You, X.-Z. *Polyhedron* **1996**, *15*, 535.
- [19] Zhang, H. -X.; Kang, B. -S.; Zhou, Z. -Y.; Chan, A. C.; Yu, K. -B. Chen, Z. -N.; Ren, C. *Inorg. Chem. Commun.* **2001**, *4*, 695.



CHAPTER II

Supramolecules Self-Assembled by Copper(II) Macrocycles with Muconic acid

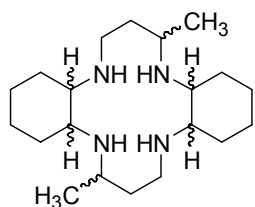
Abstract

Two new macrocyclic copper(II) supramolecules, $[\text{Cu}(\mathbf{L1})(\text{H}_2\text{O})] \cdot (\text{muco}^{2-}) \cdot (\text{H}_2\text{O})_4$ (**2**), $[\text{Cu}(\mathbf{L2})(\text{H}_2\text{O})] \cdot (\text{muco}^{2-}) \cdot (\text{H}_2\text{O})_7$ (**3**) ($\mathbf{L} = 3,14\text{-dimethyl-}2,6,13,17\text{-tetraazatricyclo}[14.4.0^{1.18}.0^{7.12}]\text{docosane}$, $\text{H}_2\text{muco} = \textit{trans,trans}$ -muconic acid) have been synthesized and structurally characterized by a combination of analytical, spectroscopies and X-ray crystallography. In **2** and **3** the structures exhibit 1D supramolecular chain containing copper(II) macrocycles which coordinated axially by one aqua ligand, uncoordinated muco^{2-} and water molecules, respectively, where the 1D chains are interconnected through hydrogen bonds by the mediation of lattice water molecules to form 2D supramolecules. Although complexes **2** and **3** show similar structures, the arrangement in which formed 1D chain are different. The introduction of diastereomerically related macrocycles **L1** and **L2** is believed to cause different arrangement in **2** and **3**.

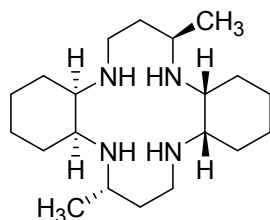
Introduction

Metallaosupramolecules consisted of transition metal ions, and ligands with intermolecular interactions such as hydrogen bond, C-H \cdots π interactions, $\pi\cdots\pi$ interactions, etc., and therefore are of interest due to their structural diversities and potential applications [1]. Metallomacrocycles **L** have 16 diastereoisomers, of which **L1** and **L2**, which have two *cis*- or *trans*-fused cyclohexane rings on a cyclam have been shown to be good building blocks with multidentate carboxylic acid for the construction of metallosupramolecules [2-8]. Although **L1** and **L2** have similar energy levels, two cyclohexane rings in which macrocycles **L1** are *cis*-fused in cyclam have various structures compared to the macrocycles **L2**, due to their different coordination environment and chemical properties [2-4,9,10]. So several metal complexes with their interesting structural features have been reported with the macrocycle **L1** rather than the macrocycle **L2** [2,3,10]. Structural differences between the two isomers are explained not only the hydrogen bonding environment change but also the coordination and arrangement differences.

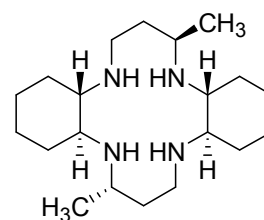
Here, the novel 1D copper(II) which were synthesized by the reaction between the copper(II) macrocyclic complex $[\text{Cu}(\mathbf{L1})](\text{ClO}_4)_2$ or $[\text{Cu}(\mathbf{L2})](\text{ClO}_4)_2$ with the H_2muco . In both complexes, various types of hydrogen bonding interactions play an important role in the structure of the copper(II) coordination as well as the arrangement difference. The details of the synthesis, structures and properties of **2** and **3** are discussed in this report.



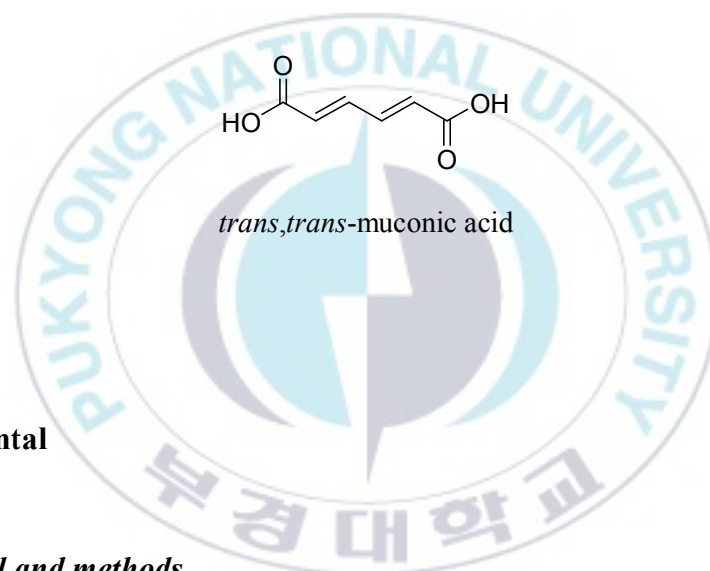
L



L1



L2



Experimental

Material and methods

All chemicals utilized in this investigation were obtained from commercial sources and were used without further purification. Distilled water used for all procedures. Infrared spectrum of solid sample was recorded on JASCO FT-IR-4000 spectrophotometer between 4000 and 400 cm^{-1} as Nujol mulls on KBr discs. Electronic spectrum using sample diluted with DMF was recorded with a Shimadzu UV-2600 recording spectrophotometer. Elemental analyses were performed on

VarioMICRO. The precursor complexes [Cu(L1)](ClO₄)₂ and [Cu(L2)](ClO₄)₂ were synthesized by previously reported methods [9].

Synthesis of 2

To a mixture of DMF and acetonitrile (1:1 v/v) solution (30 mL) of [Cu(L1)](ClO₄)₂ (240 mg, 0.4 mmol) was added an aqueous solution of H₂muco (57 mg, 0.4 mmol) and five pipette drops of triethylamine in an open beaker at ambient condition. Purple crystals of **2** were obtained in a few days. Suitable crystals of **2** for X-ray diffraction studies and subsequent spectroscopic measurements were manually collected under the microscope. Anal. Calc. for C₂₆H₅₄CuN₄O₉ (**2**): C, 49.54 %; H, 8.64 %; N, 8.89 %. Found: C, 52.27 %; H, 4.771 %; N, 8.31 %.

Synthesis of 3

To a mixture of DMF and acetonitrile (1:1 v/v) solution (20 mL) of [Cu(L2)](ClO₄)₂ (240 mg, 0.4 mmol) was added an aqueous solution of H₂muco (57 mg, 0.4 mmol) and five pipette drops of triethylamine in an open beaker at ambient condition. Purple crystals of **3** were obtained in a few days. Suitable crystals of **3** for X-ray diffraction studies and subsequent spectroscopic measurements were manually collected under the microscope. Anal. Calc. for C₂₆H₆₀CuN₄O₁₂ (**3**): C, 45.63 %; H, 8.84 %; N, 8.19%. Found: C, 45.83 %; H, 6.53 %; N, 7.08 %.

X-ray crystallography

A summary of selected crystallographic data for **2** and **3** are given in Table 2.1. X-ray data were collected on a Nonius Kappa CCD diffractometer, using graphite monochromated Mo K α radiation ($\lambda=0.71073$ Å). A combination of $1^\circ\Phi$ and Ω (with κ offsets) scans were used to collect sufficient data. The data frames were integrated and scaled using the DENZO-SMN package. The structure was solved and refined using the SHELXTL-2014/7 package. Refinement was by full-matrix least squares on F^2 , using all data (negative intensities included). Hydrogen atoms were included in calculated position.

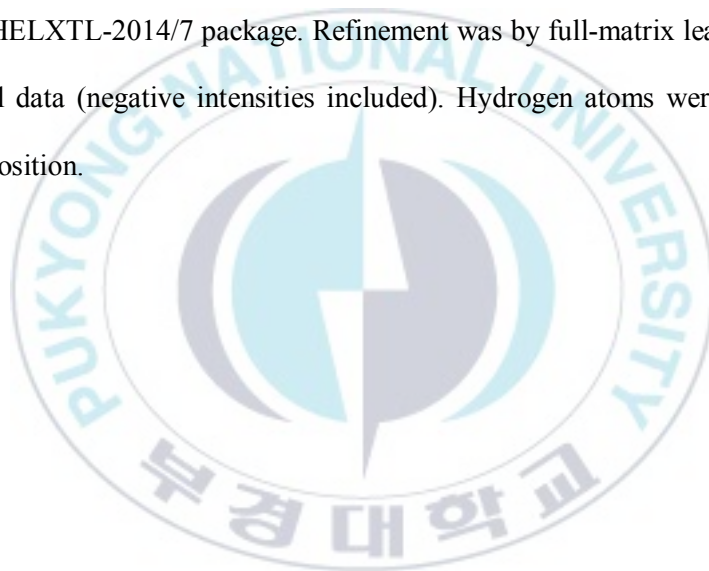


Table 2.1. Crystal data and structure refinement parameters of [Cu(L1)(H₂O)]·(muco²⁻)·(H₂O)₄ (**2**) and [Cu(L2)(H₂O)]·(muco²⁻)·(H₂O)₇ (**3**)

	2	3
Empirical formula	C ₂₆ H ₅₄ Cu N ₄ O ₉	C ₂₆ H ₆₀ Cu N ₄ O ₁₂
Formula weight	630.27	684.32
Temperature (K)	150(2)	150(2)
Wavelength (Å)	0.71073	0.71073
Crystal system	Monoclinic	Triclinic
Space group	Pc	P1
a (Å)	9.5244(7)	8.4016(8)
b (Å)	7.3656(5)	10.0721(9)
c (Å)	21.1114(15)	10.2487(9)
α (°)	90	88.833(3)
β (°)	96.983(2)	87.942(3)
γ (°)	90	73.946(2)
Volume (Å ³)	1470.04(18)	832.85(13)
Z	2	1
D _{calc.} (Mg/m ³)	1.424	1.364
Absorption coefficient (mm ⁻¹)	0.800	0.719
Crystal size (mm ³)	0.300 x 0.240 x 0.100	0.330 x 0.320 x 0.150
θ range for data collection	1.944 to 27.620°	1.988 to 27.529°
Index ranges	-12 ≤ h ≤ 12 -9 ≤ k ≤ 9 -27 ≤ l ≤ 27	-10 ≤ h ≤ 10 -13 ≤ k ≤ 13 -27 ≤ l ≤ 27
Reflections collected	22479	22084
Independent reflections	6612 [R(int) = 0.0404]	7594 [R(int) = 0.0335]
Completeness to θ	100.0 % (θ = 25.242°)	100.0 % (θ = 25.242°)
Absorption correction	Semi-empirical from equivalents	Semi-empirical from equivalents
Max. and min. transmission	0.7456 and 0.6892	0.7456 and 0.6808
Data / restraints / parameter	6612 / 2 / 362	7594 / 3 / 395
Goodness-of-fit on F ²	1.022	1.038
Final R indices [I > 2σ(I)]	R1 = 0.0343 wR2 = 0.0779	R1 = 0.0230 wR2 = 0.0591
R indices (all data)	R1 = 0.0417 wR2 = 0.0813	R1 = 0.0243 wR2 = 0.0598
Largest diff. peak and hole	0.621 and -0.322 e.Å ⁻³	0.271 and -0.199 e.Å ⁻³

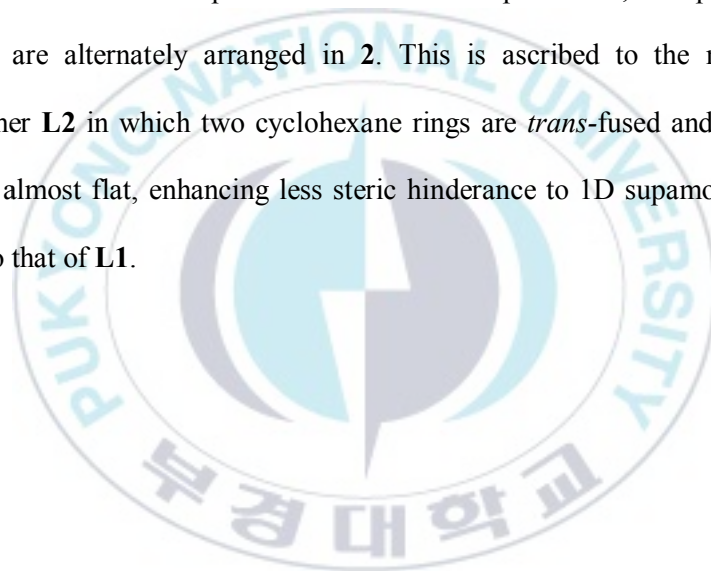
Results and Discussion

Descriptions of structures of 2 and 3

The similar complexes **2** and **3** were obtained by reacting two copper (II) complexes [Cu(**L1**)](ClO₄)₂ and [Cu(**L2**)](ClO₄)₂ with *trans/trans*-muconic acid in DMF/H₂O/CH₃CN, As shown in Figure 2.1 and Figure 2.5, the structure of **2** and **3** are composed of copper(II) macrocycles, uncoordinated muco²⁻ and some water molecules. In both of the complexes, the coordination environment around copper(II) ion exhibits a five-coordinate square pyramid with four Cu-N and one Cu-O (aqua) contacts. In **2** the four Cu-N bond distances are in the range 2.018(5) – 2.056(3) Å and longer than the Cu-O distance of 2.332(3) Å and in **3**, the four Cu-N bond distances are in the range 2.018(5) – 2.053(2) Å and longer than the Cu-O distance of 2.3711(17) Å. These values fall within the range of comparable reports for such as geometry ([Cu(**L3**)(H₂O)](O₂CCH=CHCO₂)·H₂O; Cu-N = 2.010(2) Å, 2.017(2) Å, [Cu₂(*trans*-oxap)(suc)(H₂O)]; Cu-O₄W = 2.381(2) Å, **L3** = 3,10-bis(2-hydroxyethyl)-1,3,5,8,10,12-hexaazacyclotetradecane, oxap = N,N-bis(2-aminopropyl)oxamid, suc = succinate) [11,12]. Selected bond distances and angles are given in Table 2.2 and Table 2.4. As is usual, the macrocycle in **1, 2** adopt the *trans* III (R,R,S,S,) conformation. Both of the complexes, the hydrogen bond between pre-organized N-H groups of the macrocycle and oxygen atoms of the muco²⁻, resulting in the formation a 1D supramolecular chain (Figure 2.3, Figure 2.7, Table

2.3, Table 2.5).

One of the important structural features found in both of complexes are water molecules mediate hydrogen bonding interaction between the 1D chain (Table 2.3, Table 2.5). Through these hydrogen bonding interaction the complex **2** extends its structure to form a 2D supramolecular sheets and layers (Figure 2.3, Figure 2.4, Figure 2.7, Figure 2.8). However, the different from the two complexes is the arrangement method of 1D supamolucular chain. Compared to **3**, the up form and the down form are alternately arranged in **2**. This is ascribed to the nature of the diastereoisomer **L2** in which two cyclohexane rings are *trans*-fused and shape of the macrocycle almost flat, enhancing less steric hinderance to 1D supamolucular chain compared to that of **L1**.



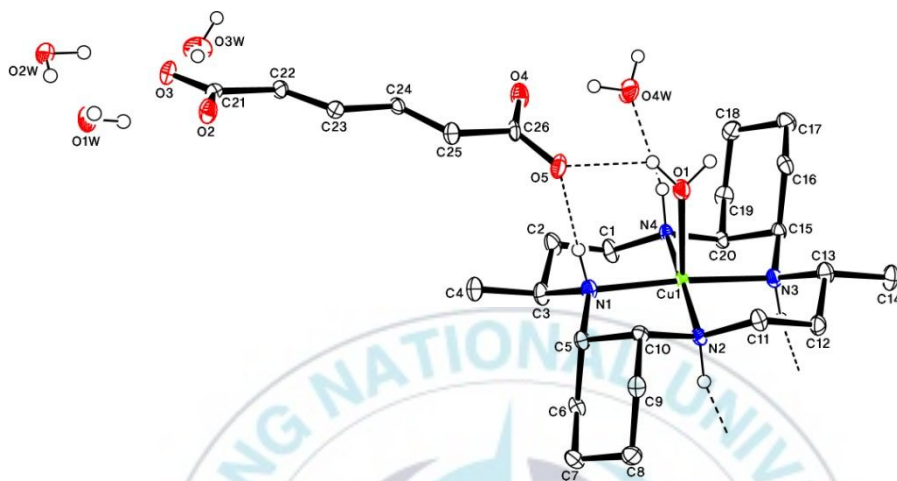


Figure 2.1. Molecular structure of $[\text{Cu}(\text{L1})(\text{H}_2\text{O})] \cdot (\text{muco}^{2-}) \cdot (\text{H}_2\text{O})_4$ (**2**) with atom-labeling scheme. Hydrogen atoms other than those participating in hydrogen bonding are omitted for clarity.

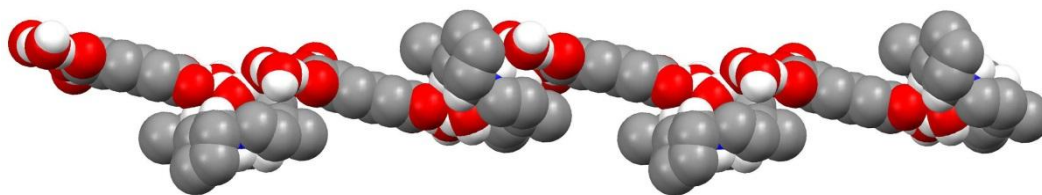


Figure 2.2. Space-filling diagram of $[\text{Cu}(\text{L1})(\text{H}_2\text{O})] \cdot (\text{muco}^{2-}) \cdot (\text{H}_2\text{O})_4$ (**2**).

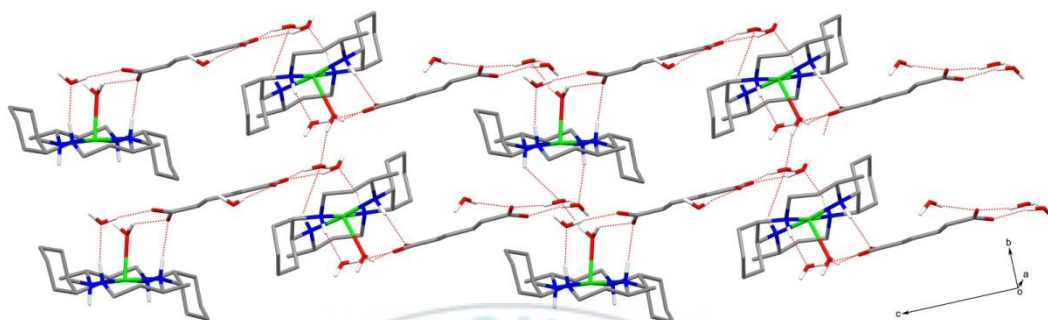


Figure 2.3. 2D supramolecular sheet of $[\text{Cu}(\text{L1})(\text{H}_2\text{O})] \cdot (\text{muco}^{2-}) \cdot (\text{H}_2\text{O})_4$ (**2**) with atom-labeling scheme. Hydrogen atoms other than those participating in hydrogen bonding are omitted for clarity.

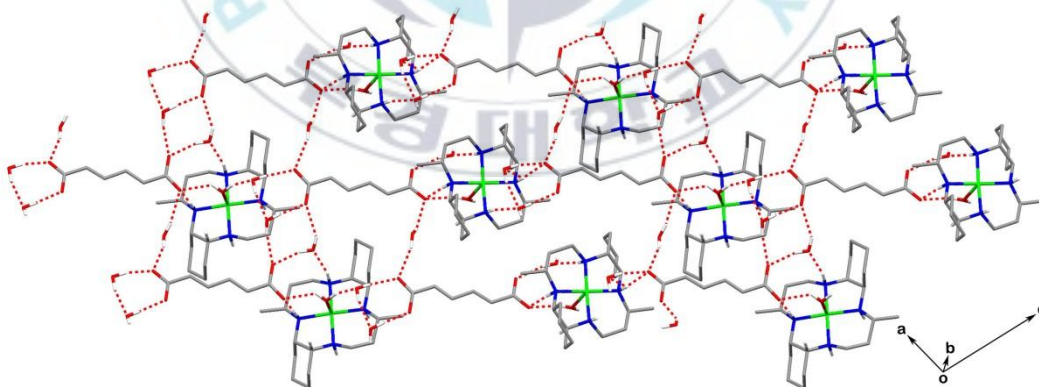


Figure 2.4. 2D supramolecular layer of $[\text{Cu}(\text{L1})(\text{H}_2\text{O})] \cdot (\text{muco}^{2-}) \cdot (\text{H}_2\text{O})_4$ (**2**) with atom-labeling scheme. Hydrogen atoms other than those participating in hydrogen bonding are omitted for clarity.

Table 2.2. Selected bond distances (Å) and angles (°) for [Cu(L1)(H₂O)]·(muco²⁻)·(H₂O)₄ (**2**)

Cu(1)-N(4)	2.018(5)	Cu(1)-N(2)	2.041(5)
Cu(1)-N(3)	2.048(3)	Cu(1)-N(1)	2.056(3)
Cu(1)-O(1)	2.332(3)		
N(4)-Cu(1)-N(3)	85.04(17)	N(2)-Cu(1)-N(3)	94.50(16)
N(4)-Cu(1)-N(1)	95.33(16)	N(2)-Cu(1)-N(1)	84.72(17)
N(4)-Cu(1)-O(1)	94.70(12)	N(2)-Cu(1)-O(1)	90.25(11)
N(3)-Cu(1)-O(1)	98.89(13)	N(1)-Cu(1)-O(1)	85.81(13)

Symmetry transformations used to generate equivalent atoms:

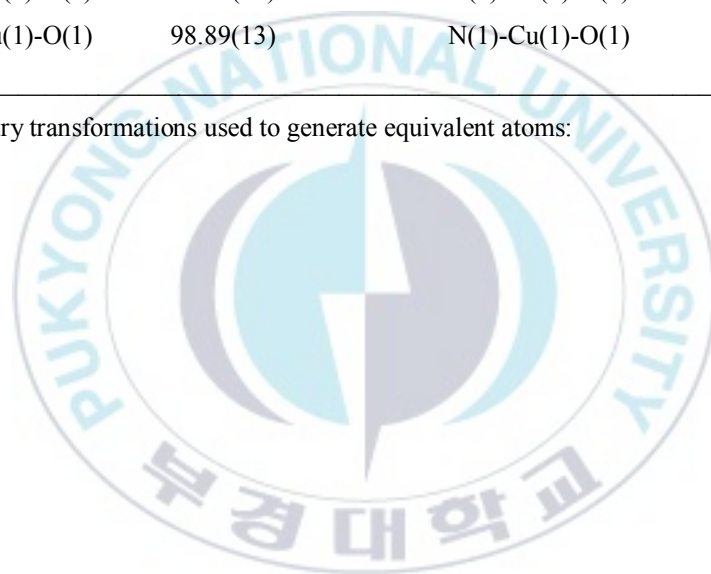


Table 2.3. Hydrogen bonds for [Cu(L1)(H₂O)]·(muco²⁻)-(H₂O)₄ (**2**) [Å and °]

D-H...A	d(D-H)	d(H...A)	d(D...A)	<(DHA)
O(1)-H(1O)...O(2W)#1	0.84	1.98	2.778(3)	158.0
O(1)-H(2O)...O(5)	0.84	2.05	2.699(4)	133.2
N(1)-H(1C)...O(5)	1.00	2.08	3.082(5)	176.1
N(2)-H(2C)...O(1W)#2	1.00	2.43	3.396(5)	162.8
N(3)-H(3B)...O(3)#2	1.00	2.19	3.163(5)	164.7
N(3)-H(3B)...O(2W)#2	1.00	2.66	3.317(5)	123.7
N(4)-H(4D)...O(4W)	1.00	2.30	3.279(5)	166.6
O(1W)-H(1WA)...O(2)	0.84	1.91	2.735(4)	168.5
O(1W)-H(1WB)...O(4)#3	0.84	2.03	2.858(5)	169.1
O(2W)-H(2WA)...O(3)	0.84	1.87	2.695(4)	165.2
O(2W)-H(2WB)...O(1W)	0.84	1.97	2.793(5)	165.0
O(3W)-H(3WA)...O(5)#4	0.84	2.30	3.028(5)	145.6
O(3W)-H(3WB)...O(3)	0.84	2.13	2.946(5)	163.3
O(4W)-H(4WA)...O(4)	0.84	1.98	2.795(4)	162.8
O(4W)-H(4WB)...O(2)#5	0.84	2.24	2.988(4)	148.1

Symmetry transformations used to generate equivalent atoms:

#1 $x-1, -y+2, z+1/2$ #2 $x-1, -y+1, z+1/2$ #3 $x, -y+2, z-1/2$ #4 $x+1, y, z$

#5 $x, -y+2, z+1/2$

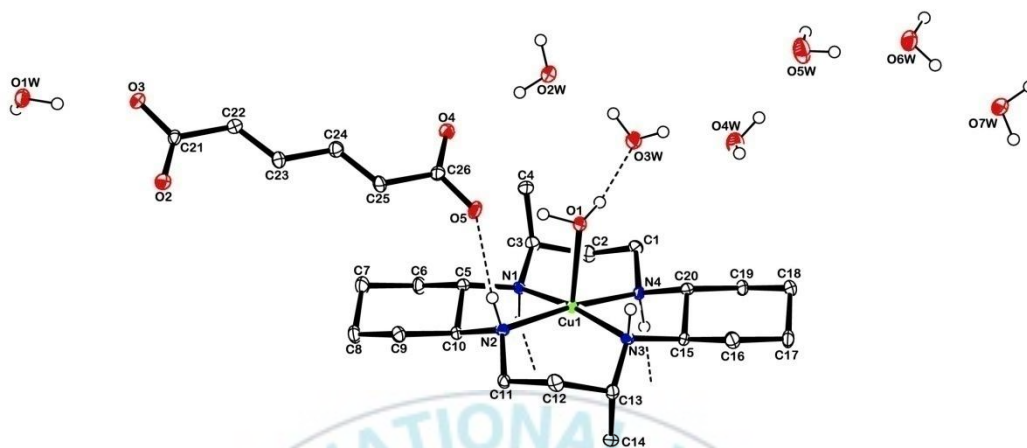


Figure 2.5. Molecular structure of $[\text{Cu}(\text{L}2)(\text{H}_2\text{O})] \cdot (\text{muco}^{2-}) \cdot (\text{H}_2\text{O})_7$ (**3**) with atom-labeling scheme. Hydrogen atoms other than those participating in hydrogen bonding are omitted for clarity.

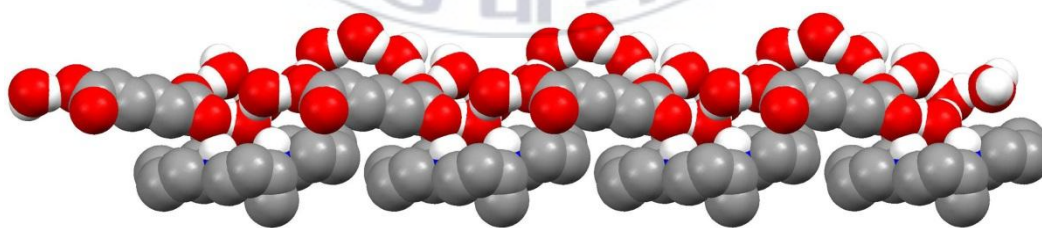


Figure 2.6. Space-filling diagram of $[\text{Cu}(\text{L}2)(\text{H}_2\text{O})] \cdot (\text{muco}^{2-}) \cdot (\text{H}_2\text{O})_7$ (**3**).

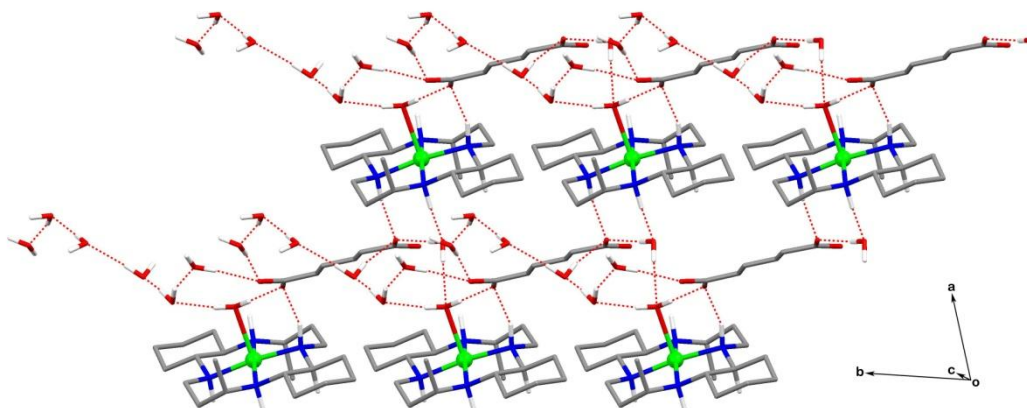


Figure 2.7. 2D supramolecular sheet of $[\text{Cu}(\text{L2})(\text{H}_2\text{O})] \cdot (\text{muco}^{2-}) \cdot (\text{H}_2\text{O})_7$ (**3**) with atom-labeling scheme. Hydrogen atoms other than those participating in hydrogen bonding are omitted for clarity.

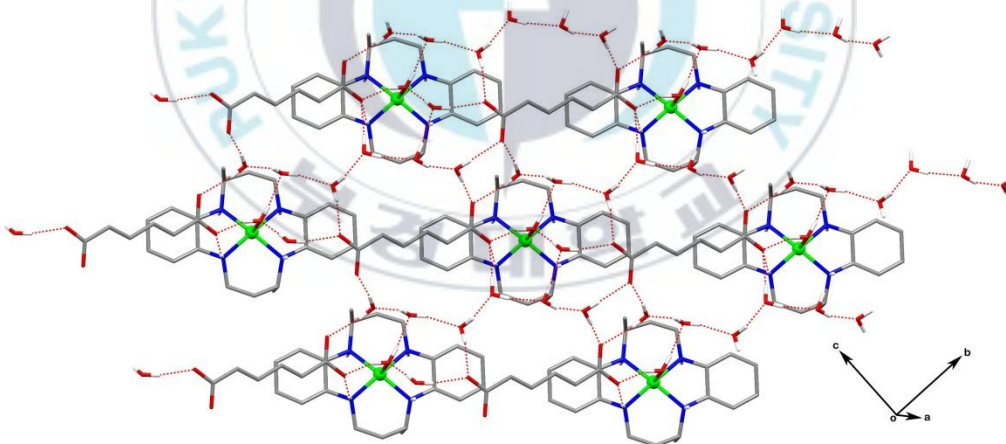


Figure 2.8. 2D supramolecular layer of $[\text{Cu}(\text{L1})(\text{H}_2\text{O})] \cdot (\text{muco}^{2-}) \cdot (\text{H}_2\text{O})_4$ (**3**) with atom-labeling scheme. Hydrogen atoms other than those participating in hydrogen bonding are omitted for clarity.

Table 2.4. Selected bond distances (Å) and angles (°) for [Cu(L2)(H₂O)]·(muco²⁻)·(H₂O)₇ (**3**)

Cu(1)-N(4)	2.018(5)	Cu(1)-N(2)	2.032(2)
Cu(1)-N(3)	2.042(2)	Cu(1)-N(1)	2.053(2)
Cu(1)-O(1)	2.3711(17)		
N(4)-Cu(1)-N(1)	94.08(9)	N(1)-Cu(1)-N(2)	84.37(9)
N(4)-Cu(1)-N(3)	84.52(9)	N(2)-Cu(1)-N(3)	95.82(9)
N(4)-Cu(1)-O(1)	96.46(8)	N(2)-Cu(1)-O(1)	90.93(8)
N(3)-Cu(1)-O(1)	83.64(7)	N(1)-Cu(1)-O(1)	105.82(8)

Symmetry transformations used to generate equivalent atoms:

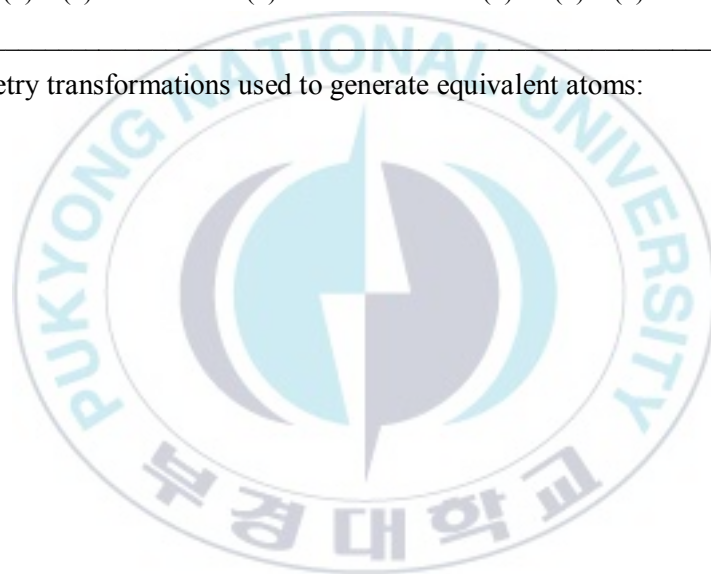


Table 2.5. Hydrogen bonds for for [Cu(L2)(H₂O)]·(muco²⁻)·(H₂O)₇ (**3**) [Å and °]

D-H...A	d(D-H)	d(H...A)	d(D...A)	<(DHA)
O(1)-H(1O)...O(3W)	0.81(3)	1.89(3)	2.686(3)	166(3)
O(1)-H(2O)...O(5)	0.91(3)	1.77(3)	2.649(3)	160(3)
N(1)-H(1C)...O(1W)#1	1.00	2.10	3.016(3)	151.8
N(2)-H(2B)...O(5)	1.00	2.19	3.129(3)	156.4
N(4)-H(4D)...O(3)#1	1.00	2.06	3.053(3)	169.4
O(1W)-H(1WA)...O(1)#2	0.84	2.05	2.891(2)	176.9
O(1W)-H(1WB)...O(3)	0.84	1.89	2.717(3)	168.3
O(2W)-H(2WA)...O(2)#3	0.84	1.96	2.797(3)	172.1
O(2W)-H(2WB)...O(4)	0.84	1.99	2.821(3)	171.2
O(3W)-H(3WA)...O(2W)	0.84	1.89	2.693(3)	159.3
O(3W)-H(3WB)...O(4W)	0.84	1.92	2.712(3)	157.2
O(4W)-H(4WA)...O(3)#4	0.84	1.96	2.791(3)	168.1
O(4W)-H(4WB)...O(5W)	0.84	1.89	2.719(3)	167.8
O(5W)-H(5WA)...O(5)#3	0.84	1.93	2.762(3)	173.8
O(5W)-H(5WB)...O(6W)	0.84	1.90	2.727(3)	169.9
O(6W)-H(6WA)...O(7W)	0.84	1.92	2.729(3)	162.1
O(6W)-H(6WB)...O(1W)#5	0.84	1.96	2.798(3)	174.7
O(7W)-H(7WA)...O(4)#4	0.84	1.96	2.786(3)	168.0
O(7W)-H(7WB)...O(2)#5	0.84	1.99	2.819(3)	168.0

Symmetry transformations used to generate equivalent atoms:

#1 x-1,y+1,z-1 #2 x,y-1,z+1 #3 x,y+1,z #4 x,y+1,z-1

#5 x,y+2,z-1

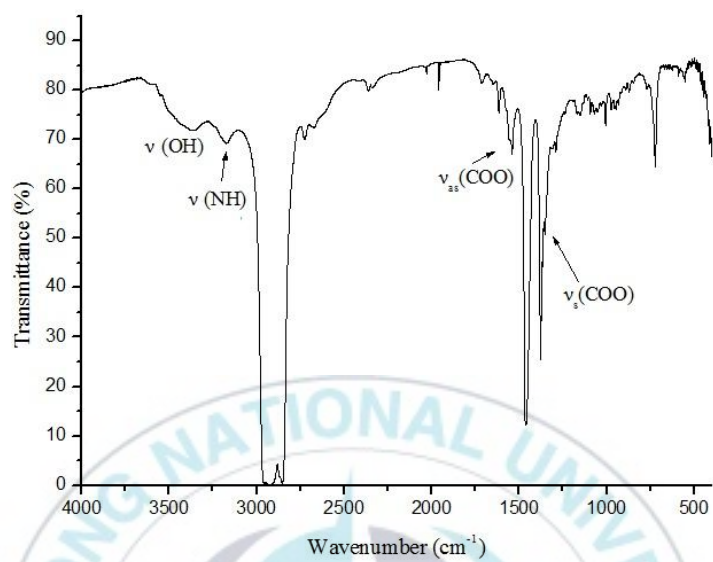
Spectroscopic properties for 2 and 3

The microanalytical results for **2** and **3** were consistent with the structures determined by X-ray diffraction methods.

The IR spectrum of **2** shows the stretching frequencies of carboxyl groups at 1615, 1544 cm^{-1} for the $\nu_{\text{as}}(\text{COO})$ and 1352, 1290 cm^{-1} for the $\nu_{\text{s}}(\text{COO})$. Similarly, the absorption bands for the carboxyl groups at 1611, 1588 cm^{-1} for the $\nu_{\text{as}}(\text{COO})$ and 1349, 1287 cm^{-1} for the $\nu_{\text{s}}(\text{COO})$ are observed in **3**. In addition, weak bands $\nu(\text{OH})$ at 3352 and 3233 cm^{-1} in **2** (3356 and 3240 cm^{-1} in **3**) and weak band $\nu(\text{NH})$ at 3166 cm^{-1} (3168 cm^{-1} in **2**) indicate that the complexes **2** and **3** contain a macrocyclic ligand, carboxylic acid, water molecules.

The solid state electronic spectrum of **2** and **3** are composed of two bands at 272 and 556 nm. The broad lower energy bands in the visible region are d-d transition, are attributed to a composite of the three possible transition for d_{xy} , d_{yz} , d_{zx} to $d_{x^2-y^2}$. The strong higher energy bands are assigned to ligand-metal charge transfer transitions related axial oxygen or macrocycle nitrogen donors.

(a)



(b)

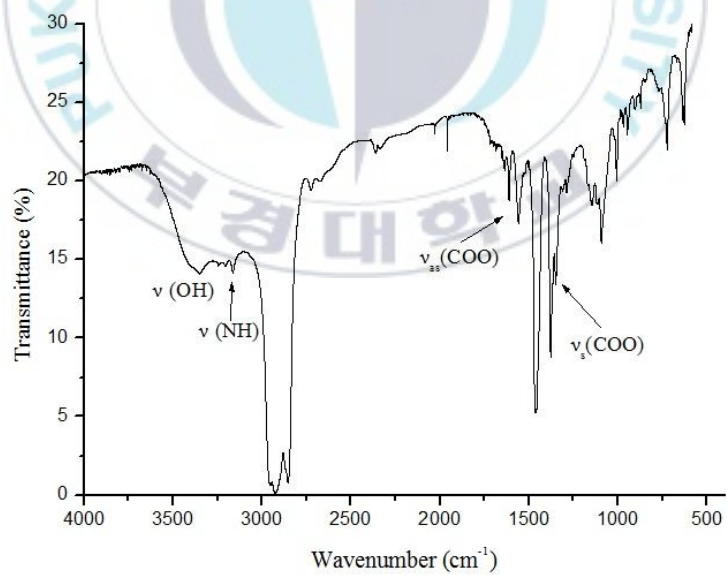
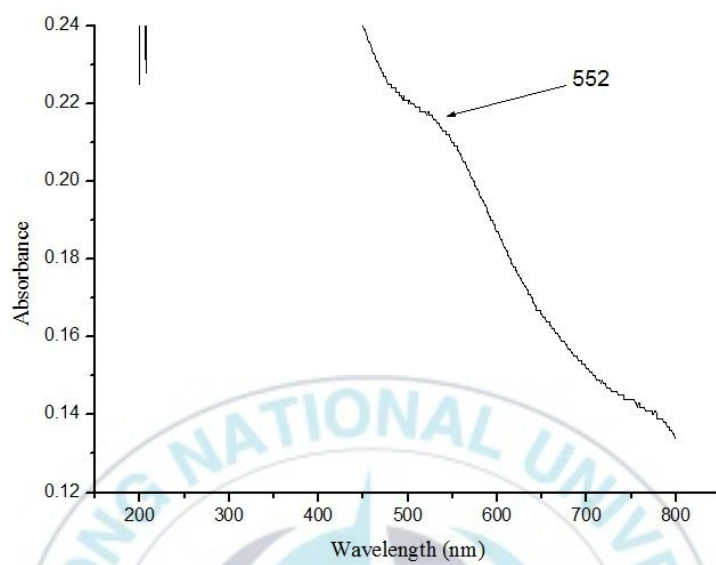


Figure 2.9. Infrared spectra of (a) $[\text{Cu}(\text{L1})(\text{H}_2\text{O})] \cdot (\text{muco}^{2-}) \cdot (\text{H}_2\text{O})_4$ (**2**) and (b) $[\text{Cu}(\text{L2})(\text{H}_2\text{O})] \cdot (\text{muco}^{2-}) \cdot (\text{H}_2\text{O})_7$ (**3**) [Nujol mull].

(a)



(b)

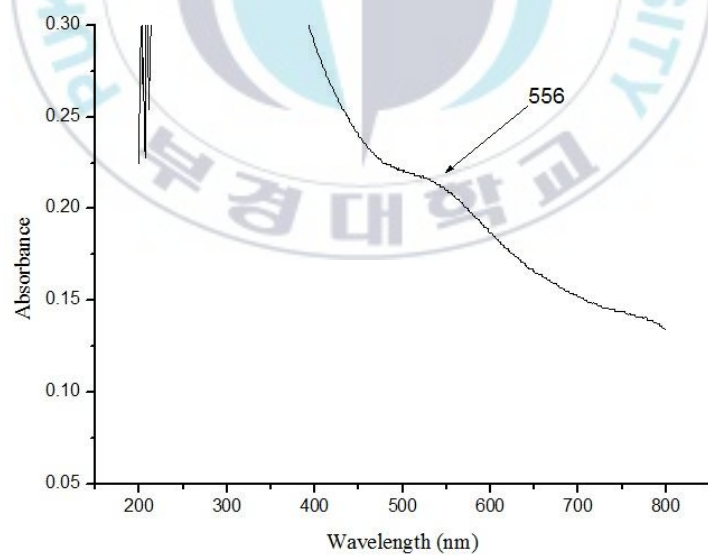


Figure 2.10. Electronic spectra for (a) $[\text{Cu}(\text{L1})(\text{H}_2\text{O})] \cdot (\text{muco}^{2-}) \cdot (\text{H}_2\text{O})_4$ (**2**) and (b) $[\text{Cu}(\text{L2})(\text{H}_2\text{O})] \cdot (\text{muco}^{2-}) \cdot (\text{H}_2\text{O})_7$ (**3**) in DMF.

References

- [1] Suh, M.P.; Cheon, Y. Y.; Lee, E. Y. *Coord. Chem. Rev.* **2008**, *252*, 1007.
- [2] Kim, J. A.; Park, H.; Kim, J. C.; Lough, A. J.; Pyun, S. Y.; Roh, J.; Lee, B. M. *Inorg. Chim. Acta* **2008**, *361*, 2087.
- [3] Park, H.; Kim, J. C.; Lough, A. J.; Lee, B. M. *Inorg. Chem. Commun.* **2007**, *10*, 303.
- [4] Kim, J. C.; Cho, J.; Lough, A. J. *Inorg. Chim. Acta* **2001**, *317*, 252.
- [5] Park, H.; Jeong, M. H.; Kim, J. C.; Lough, A. J. *Bull. Korean Chem.. Soc.* **2007**, *28*, 303.
- [6] Choi, K.-Y.; Suh, I.-H.; Kim, D. W. *Inorg. Chim. Acta* **1999**, *293*, 100.
- [7] Choi, K.-Y.; Chun, K. M.; Suh, I.-H. *Polyhedron* **2001**, *20*, 57.
- [8] Choi, K.-Y.; Lim, I.-T. *Polyhedron* **2017**, *127*, 361.
- [9] Kang, S.-G.; Kweon, J. K.; Jeong, S.-K. *Bull. Korean chem.. Soc.* **1991**, *12*, 483.
- [10] Kim, J. C.; Cho, J.; Kim, H.; Lough, A. J. *Chem. Commun.* **2004**, 1796.
- [11] Kim, J. C.; Lough, A. J. *J. Chem. Crystallogr.* **2005**, *35*, 535.
- [12] Zhang, H.-X.; Kang, B.-S.; Zhou, Z.-Y.; Chan, A.C.; Yu, K.-B.; Chen, Z.-N.; Ren, C. *Inorg. Chem. Commun.* **2001**, *4*, 695.

테트라아자 거대고리 구리(II) 착물의 합성 및 구조

김태영

부경대학교 대학원 화학과

요 약

$[\text{Cu}(\mathbf{L1})(\text{H}_2\text{O})_2][\text{Cu}_2(\mathbf{L1})_2(\mu\text{-btc}^4)] \cdot 2\text{ClO}_4 \cdot 6\text{H}_2\text{O} \cdot 1.454\text{CH}_3\text{CN}$ (**1**), $[\text{Cu}(\mathbf{L1})(\text{H}_2\text{O})] \cdot (\text{muco}^{2-}) \cdot (\text{H}_2\text{O})_4$ (**2**), $[\text{Cu}(\mathbf{L2})(\text{H}_2\text{O})] \cdot (\text{muco}^{2-}) \cdot (\text{H}_2\text{O})_7$ (**3**) ($\mathbf{L} = 3,14\text{-dimethyl-}2,6,13,17\text{-tetraazatricyclo}[14.4.0^{1.18}.0^{7.12}]\text{docosane}$, $\text{H}_4\text{btc} = 1,2,4,5\text{-benzenetetra-carboxylic acid}$, $\text{H}_2\text{muco} = \text{trans,trans-muconic acid}$)의 조성을 갖는 3개의 구리(II) 착물을 합성하였고, 원소분석, 분광학 및 X-ray 결정학적 방법을 통해 구조적인 특성을 알아 낼 수 있었다. (**1**)에서는 5배위 사각뿔과 수직방향으로 늘어난 6배위 팔면체의 2가지 다른 구리(II) 배위 기하구조를 관찰 할 수 있었고, (**2**), (**3**)에서는 유사한 구조를 가지고 있지만, 배열방식에서 차이점이 있는 것을 관찰 할 수 있었다. 다양한 형태의 수소 결합 상호작용이 구조적인 기하구조를 결정하는데 중요한 역할을 한다.

Acknowledgement

I would like to extend my special appreciation to my advisor, Prof. Ju Chang Kim, whose academic guidance made my life as well as my study a precious experience.

I would also like to thank Prof. Sang Yong Pyun and Prof. Yong-Cheol Kang for their time and comments for this thesis. I appreciate of the guidance and help of other faculties during the stay at department of chemistry at Pukyong National University. I am grateful to Dr. Alan J. Lough (University of Toronto) for solving X-ray crystallographic data.

I thank to members of Molecular Design Lab (Seonghyeok Moon, Youjeong Lee, Yujeong Kim and Suna Jang). Finally, I am really thankful to my parents and younger sister for their constant supports and thoughtfulness throughout my whole life.

